CHAPTER 3

Light Front QCD: Perturbative Structure

In the previous chapter we looked at the caconical structure of light front QCD. In this chapter we look at the perturbative structure. After discussing a tree level calculation and one loop calculation for fermion self energy we take a detailed look at coupling constant renormalization. We consider helicity flip and helicity non-flip processes separately.

3.1 Interaction Representation

To facilitate perturbative calculations, we go to the interaction representation. In interaction representation, the equations of motion for the field operators are

$$i\partial^- \eta(x) = [\eta(x), P_0^-] \tag{3.1}$$

and

$$i\partial^- A_a^i(x) = [A_a^i(x), P_0^-] \tag{3.2}$$

where P_0^- is the free light front Hamiltonian. The solutions are

$$\eta(x) = \sum_\lambda \chi_\lambda \int \frac{dk^+ d^2k^\perp}{2(2\pi)^3\sqrt{k^+}}[b(k,\lambda)e^{-ik.x} + d^\dagger(k,-\lambda)e^{ik.x}] \tag{3.3}$$

with $\lambda = \pm 1$, χ_λ is the Pauli spinor and

$$\{b(k,\lambda), b^\dagger(k',\lambda')\} = \{d(k,\lambda), d^\dagger(k',\lambda')\} = 2(2\pi)^3 k^+ \delta^3(k-k'). \tag{3.4}$$

and

$$A^\perp(x) = \sum_\lambda \int \frac{dk^+ d^2k^\perp}{2(2\pi)^3 k^+}[a(k,\lambda)\epsilon_\lambda^\perp e^{-ik.x} + a^\dagger(k,\lambda)(\epsilon_\lambda^\perp)^* e^{ik.x}] \tag{3.5}$$

with $\lambda = \pm 1$ and $\epsilon_1^\perp = \frac{1}{\sqrt{2}}(1,i)$ and $\epsilon_2^\perp = \frac{1}{\sqrt{2}}(1,-i)$ and

$$\{a(k,\lambda), a^\dagger(k',\lambda')\} = 2(2\pi)^3 k^+ \delta^3(k-k'). \tag{3.6}$$

3.2 Old fashioned perturbation theory for S matrix elements

Our starting point is the expression for S matrix in perturbation theory. We have

$$S = 1 - \frac{i}{2}\int_{-\infty}^{+\infty} dx^+ \; V_I(x^+) - \Big(\frac{1}{2}\Big)^2 \int_{-\infty}^{+\infty} dx_1^+ V_I(x_1^+) \int_{-\infty}^{x_1^+} dx_2^+ V_I(x_2^+) + \dots . \tag{3.7}$$

V_I is the interaction light front Hamiltonian in the interaction representation.

Let us assume that at time $x^+ = -\infty$, the system is known to be in the state $\mid \phi_i\rangle$ and at time $x^+ = +\infty$, the system is known to be in the state $\mid \phi_f\rangle$. The states $\mid \phi_i\rangle$ and $\mid \phi_f\rangle$ are eigenstates of the free light-front Hamiltonian P_0^-.

We have

$$\begin{aligned} S_{fi} \quad &= \langle \phi_f \mid S \mid \phi_i\rangle \\ &= \delta_{fi} - i\frac{1}{2}\int_{-\infty}^{+\infty} dx^+ \; \langle \phi_f \mid V_I(x^+) \mid \phi_i\rangle \\ &- \Big(\frac{1}{2}\Big)^2 \int_{-\infty}^{+\infty} dx_1^+ \langle \phi_f \mid V_I(x_1^+) \int_{-\infty}^{x_1^+} dx_2^+ V_I(x_2^+) \mid \phi_i\rangle + \dots . \end{aligned} \tag{3.8}$$

Using

$$V_I(x^+) = e^{\frac{i}{2}P_0^- x^+} V_S(0) e^{-\frac{1}{2}P_0^- x^+} \tag{3.9}$$

and inserting a complete set of states $\mid \phi_n\rangle$ in the third term, we arrive at the familiar perturbation theory formula for S-matrix elements

$$S_{fi} = \delta_{fi} - 2\pi i \delta(E_i^- - E_f^-) T_{fi} \tag{3.10}$$

where

$$T_{fi} = \langle \phi_f \mid V_S(0) \mid \phi_i\rangle \; + \; \sum_n \frac{\langle \phi_f \mid V_S(0) \mid \phi_n\rangle\langle \phi_n \mid V_S(0) \mid \phi_i\rangle}{E_i^- - E_n^- + i\epsilon} + \dots . \tag{3.11}$$

3.3 Diagrammatic rules

The vertices in light front QCD Hamiltonian are listed in the table. These are obtained by directly calculating the matrix element between free particle states. The rules to write the expression for perturbative diagrams are as follows:

1. Draw all topologically distinct x^+ ordered diagrams.

2. For each internal line, sum over the helicity and integrate using $\int \frac{dk^+ d^2k^\perp}{2(2\pi)^3 k^+}\theta(k^+)$.

3. For each vertex, include a factor of $2(2\pi)^3\delta^3(k_f - k_i)$ and a simple matrix element listed in the Table.

4. Include a factor $(k_f^- - \sum_n k_n^- + i\epsilon)^{-1}$ for each intermediate state, where $\sum_n k_n^-$ sum over all on mass-shell intermediate particle energies.

5. Add a symmetry factor S^{-1} for each gluon loop, coming from the symmetrized boson states.

x^+-ordered Hamiltonian Diagrammatic Rules:

H_{int}	Diagram	Vertex
H_{qqg}	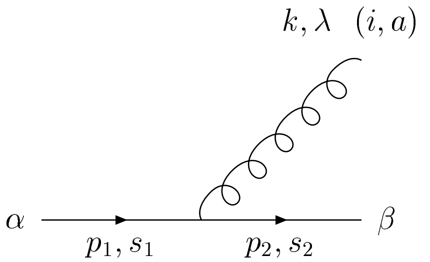	$-gT^a_{\beta\alpha}\sqrt{p_1^+}\sqrt{p_2^+}$ $\chi^\dagger_{s_2}\left\{2\frac{k^i}{[k^+]} - \frac{\sigma^\perp\cdot p_2^\perp - im}{[p_2^+]}\sigma^i - \sigma^i\frac{\sigma^\perp\cdot p_1^\perp + im}{[p_1^+]}\right\}\chi_{s_1}\epsilon^{i*}_\lambda$
H_{ggg}	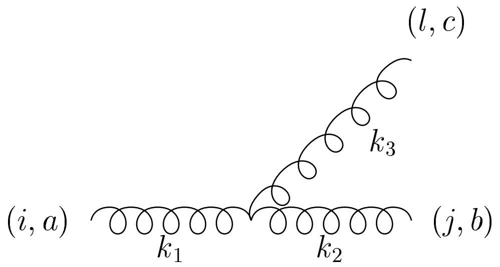	$-igf^{abc}\varepsilon^i\varepsilon^{j*}\varepsilon^{l*}\Big\{\Big[(k_2 - k_3)^i - \frac{k_1^i}{[k_1^+]}\Big(k_2^+ - k_3^+\Big)\Big]\delta_{jl}$ $+\Big[(k_3 + k_1)^j - \frac{k_2^j}{[k_2^+]}(k_3^+ + k_1^+)\Big]\delta_{li}$ $+\Big[-(k_1 + k_2)^l + \frac{k_3^l}{[k_3^+]}(k_1^+ + k_2^+)\Big]\delta_{ij}\Big\}$

H_{qqgg1}

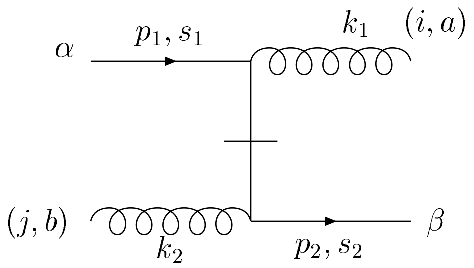

$$g^2\sqrt{p_1^+}\sqrt{p_2^+}\chi_{s_2}^\dagger\left\{\frac{(T^bT^a)_{\beta\alpha}\sigma^j\sigma^i}{[p_1^+-k_1^+]}\right\}\chi_{s_1}\epsilon^{i*}\epsilon^j$$

H_{qqgg2}

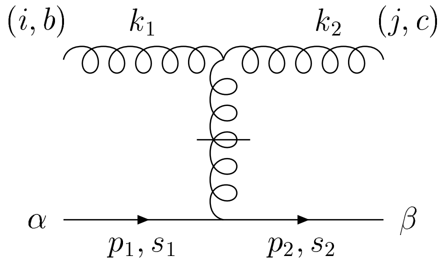

$$-2g^2\sqrt{p_1^+}\sqrt{p_2^+}iT^a_{\beta\alpha}f^{abc}\chi_{s_2}^\dagger\frac{k_1^++k_2^+}{[k_1^+-k_2^+]^2}\chi_{s_1}\delta_{ij}\epsilon^i\epsilon^{j*}$$

H_{qqqq}

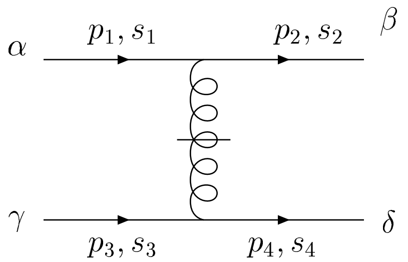

$$2g^2\sqrt{p_1^+p_2^+p_3^+p_4^+}T^a_{\beta\alpha}T^a_{\delta\gamma}$$
$$\chi_{s_2}^\dagger\chi_{s_1}\left\{\frac{1}{[p_1^+-p_2^+]^2}\right\}\chi_{s_4}^\dagger\chi_{s_3}$$

H_{gggg2}

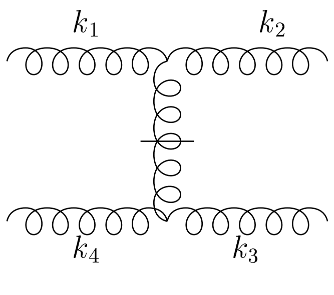

$$g^2\left\{f^{a_1a_2b}f^{a_3a_4b}\delta_{i_1i_2}\delta_{i_3i_4}\frac{(k_1^++k_2^+)(k_3^++k_4^+)}{[k_1^+-k_2^+][k_3^+-k_4^+]}\right.$$
$$\left.+(2\to3)+(2\to4)\cdot\right\}$$

H_{gggg2}

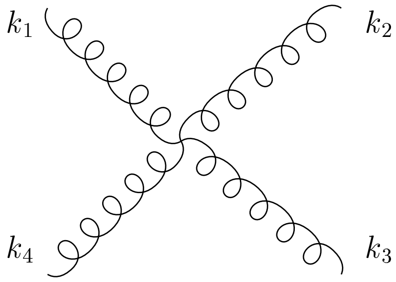

$$g^2\left\{f^{a_1a_2b}f^{a_3a_4b}\left[\delta_{i_1i_3}\delta_{i_2i_4}-\delta_{i_1i_4}\delta_{i_2i_3}\right] +(2\to 3)+(2\to 4)\right\}$$

Remarks: All gluon momenta directions are x^+ - ordered (from left to right). The indices $\alpha, \beta, ...$ corresponds to quark color and run from 1 to 3, $a, b, c, ...$ gluon color from 1 to 8, and $i, j, ...$ transverse space indices from 1 to 2. A slash on fermion line or gluon line indicates instantaneous propagation.

3.4 Example: tree level

As an example of old fashioned perturbation theory calculations, we consider qq scattering in lowest order. Starting from the light front gauge $A^+ = 0$ amplitude in the manifestly noncovariant formalism, we show how to recover the covariant amplitude in Feynman gauge.

For the sake of ease of comparison with Feynman ampitudes, it is helpful to go from the two-component form to the four-component form of the quark gluon vertex. This can be achieved as follows. We have,

$$u^+(k,s) = \begin{pmatrix} \chi_s \\ 0 \end{pmatrix}. \tag{3.12}$$

From $[\gamma^\mu k_\mu - m]u(k,s) = 0$, we get

$$u^-(k,s) = [\alpha^\perp \cdot k^\perp + \gamma^0 m]\frac{1}{k^+}u^+(k,s). \tag{3.13}$$

$u = u^+ + u^-$. Note that in $A^+ = 0$ gauge, $\epsilon_\lambda^+(k) = 0$. Consider

$$\begin{aligned} \bar{u}(p_2,\sigma_2)\gamma_\mu(\epsilon_\lambda^\mu)^*(q)u(p_1,\sigma_1) \quad &= (u^+)^\dagger(p_2,\sigma_2){\epsilon_\lambda^-}^*(q)u^+(p_1,\sigma_1) \\ &\quad - (u^+)^\dagger(p_2,\sigma_2)\alpha^\perp\cdot(\epsilon_\lambda^\perp)^*(q)u^-(p_1,\sigma_1) \\ &\quad - (u^-)^\dagger(p_2,\sigma_2)\alpha^\perp\cdot(\epsilon_\lambda^\perp)^*(q)u^+(p_1,\sigma_1) \end{aligned} \tag{3.14}$$

We have,

$$
\begin{aligned}
(u^+)^\dagger(p_2,\sigma_2)\epsilon_\lambda^{-*}(q)u^+(p_1,\sigma_1) \quad &= (u^+)^\dagger(p_2,\sigma_2)2\frac{q^\perp}{q^+}\cdot(\epsilon_\lambda^\perp)^*(q)u^+(p_1,\sigma_1) \\
&= \chi_{\sigma_2}^\dagger 2\frac{q^\perp}{q^+}\chi_{\sigma_1}, \\
(u^+)^\dagger(p_2,\sigma_2)\alpha^\perp\cdot(\epsilon_\lambda^\perp)^*(q)u^-(p_1,\sigma_1) \quad &= \chi_{\sigma_2}^\dagger\Big[\hat\sigma^\perp\frac{\hat\sigma^\perp\cdot p_1^\perp}{p_1^+} + i\frac{m}{p_1^+}\hat\sigma^\perp\Big]\chi_{\sigma_1}\cdot(\epsilon_\lambda^\perp)^*, \\
(u^-)^\dagger(p_2,\sigma_2)\alpha^\perp\cdot(\epsilon_\lambda^\perp)^*(q)u^+(p_1,\sigma_1) \quad &= \chi_{\sigma_2}^\dagger\Big[\frac{\hat\sigma^\perp\cdot p_2^\perp}{p_2^+}\hat\sigma^\perp - i\frac{m}{p_2^+}\hat\sigma^\perp\Big]\chi_{\sigma_1}\cdot(\epsilon_\lambda^\perp)^*. \quad (3.15)
\end{aligned}
$$

Thus we have the short hand notation in the four component form,

$$
\bar u(p_2,\sigma_2)\gamma_\mu(\epsilon_\lambda^\mu)^*(q)u(p_1,\sigma_1) = \chi_{\sigma_2}^\dagger\Big[\frac{2q^i}{q^+} - \frac{\sigma^\perp.p_2^\perp}{p_2^+}\sigma^i - \sigma^i\frac{\sigma^\perp.p_1^\perp}{p_1^+} + im(\frac{1}{p_2^+}-\frac{1}{p_1^+})\sigma^i\Big]\chi_{\sigma_1}\,\epsilon_\lambda^{i*}. \tag{3.16}
$$

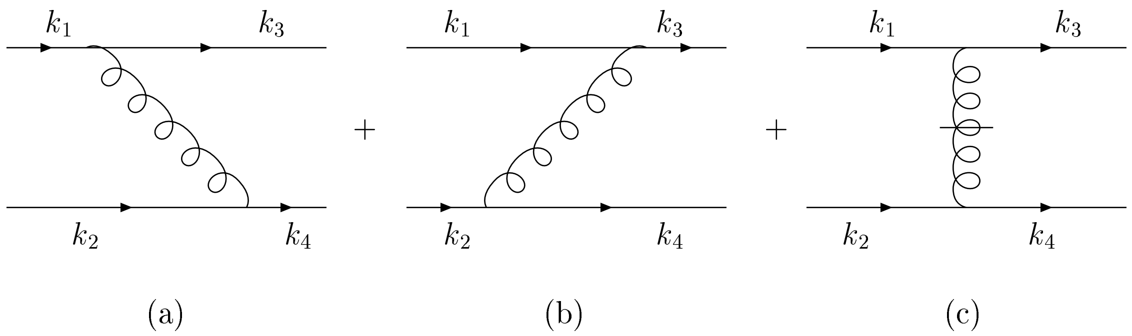

Fig. 3

The instantaneous interaction contribution is given by (see Fig. 3.c)

$$
\begin{aligned}
T_{fi(inst)} \quad &= 4g^2T^aT^a\sqrt{k_1^+k_2^+k_3^+k_4^+}\chi_{\sigma_3}^\dagger\chi_{\sigma_1}\chi_{\sigma_4}^\dagger\chi_{\sigma_2}\frac{1}{(k_1^+-k_3^+)^2} \\
&= g^2T^aT^a\sqrt{k_1^+k_2^+k_3^+k_4^+}\frac{\bar u(k_3,\sigma_3)\gamma^+u(k_1,\sigma_1)\bar u(k_4,\sigma_4)\gamma^+u(k_2,\sigma_2)}{(k_1^+-k_3^+)^2}. \quad (3.17)
\end{aligned}
$$

The second order time ordered contributions are (Fig. 3.a-b)

$$
T_{fi(to)} \quad = g^2T^aT^a\sqrt{k_1^+k_2^+k_3^+k_4^+}
$$

$$\sum_\lambda \bar{u}(k_3,\sigma_3)\gamma^\mu(\epsilon_{\lambda\mu})^*(k_1-k_3)u(k_1,\sigma_1)\bar{u}(k_4,\sigma_4)\gamma^\nu(\epsilon_{\lambda\nu})(k_1-k_3)u(k_2,\sigma_2)$$
$$\Big[\frac{\theta(k_1^+-k_3^+)}{(k_1^+-k_3^+)}\frac{1}{P^- - k_3^- - k_2^- - \frac{(k_1^\perp-k_3^\perp)^2}{k_1^+-k_3^+}+i\epsilon}$$
$$+\frac{\theta(k_3^+-k_1^+)}{(k_3^+-k_1^+)}\frac{1}{P^- - k_1^- - k_4^- - \frac{(k_3^\perp-k_1^\perp)^2}{k_3^+-k_1^+}+i\epsilon}\Big]. \tag{3.18}$$

With $\eta^\mu = (2,0,0^\perp)$ so that $\eta\cdot k = k^+$, we have,

$$\sum_\lambda(\epsilon_{\lambda\mu})^*(k_1-k_3)\epsilon_{\lambda\nu}(k_1-k_3) = -g_{\mu\nu} + \frac{\eta_\mu(k_1-k_3)_\nu}{k_1^+-k_3^+} + \frac{\eta_\nu(k_1-k_3)_\mu}{k_1^+-k_3^+}. \tag{3.19}$$

For the S matrix element, we have the overall energy conservation $P^- = k_1^- + k_2^- = k_3^- + k_4^-$. Then the terms inside the square bracket becomes

$$\frac{\theta(k_1^+-k_3^+)}{(k_1^+-k_3^+)}\frac{1}{k_1^- - k_3^- - \frac{(k_1^\perp-k_3^\perp)^2}{k_1^+-k_3^+}+i\epsilon}$$
$$+\frac{\theta(k_3^+-k_1^+)}{(k_3^+-k_1^+)}\frac{1}{k_3^- - k_1^- - \frac{(k_3^\perp-k_1^\perp)^2}{k_3^+-k_1^+}+i\epsilon}$$
$$= \frac{1}{(k_1^+-k_3^+)(k_1^- - k_3^-) - (k_1^\perp-k_3^\perp)^2 + i\epsilon}. \tag{3.20}$$

Thus the second order S matrix element for qq scattering is

$$S_{fi} = g^2T^aT^a\sqrt{k_1^+k_2^+k_3^+k_4^+}\,\bar{u}(k_3,\sigma_3)\gamma^\mu u(k_1,\sigma_1)\bar{u}(k_4,\sigma_4)\gamma^\nu u(k_2,\sigma_2)\frac{-g_{\mu\nu}}{q^2+i\epsilon} \quad + \text{rest}. \tag{3.21}$$

We have introduced the four vector $q = k_1 - k_3$ which is not on shell. We proceed to show that the terms denoted by "rest" is zero.

Using $\gamma^\mu\eta_\mu = \gamma^+$, we have, apart from common factors, the "rest" =

$$\frac{\bar{u}(k_3,\sigma_3)\gamma^+u(k_1,\sigma_1)}{k_1^+-k_3^+}\Big[\frac{\bar{u}(k_4,\sigma_4)\gamma^\nu u(k_2,\sigma_2)}{(k_1^+-k_3^+)(k_1^- - k_3^-) - (k_1^\perp-k_3^\perp)^2+i\epsilon}(k_1-k_3)_\nu$$
$$+\frac{1}{2}\frac{\bar{u}(k_4,\sigma_4)\gamma^+u(k_2,\sigma_2)}{k_1^+-k_3^+}\Big]$$
$$+\frac{\bar{u}(k_4,\sigma_4)\gamma^+u(k_2,\sigma_2)}{k_1^+-k_3^+}\Big[\frac{\bar{u}(k_3,\sigma_3)\gamma^\mu u(k_1,\sigma_1)}{(k_1^+-k_3^+)(k_1^- - k_3^-) - (k_1^\perp-k_3^\perp)^2+i\epsilon}(k_1-k_3)_\mu$$
$$+\frac{1}{2}\frac{\bar{u}(k_3,\sigma_3)\gamma^+u(k_1,\sigma_1)}{k_1^+-k_3^+}\Big] \tag{3.22}$$

The term inside the first square bracket is $\frac{\bar{u}(k_4,\sigma_4)(\gamma^\mu k_{1\mu} - \gamma^\mu k_{3\mu})u(k_2,\sigma_2)}{q^2+i\epsilon}$. Since $k_1 - k_3 = k_4 - k_2$, we get $\bar{u}(k_4,\sigma_4)(\gamma^\mu k_{4\mu} - \gamma^\mu k_{2\mu})u(k_2,\sigma_2) = 0$. Similarly the second term also is zero. Thus we have shown that the second order S matrix element for qq scattering calculated in light front time orderd perturbation theory in the gauge $A^+ = 0$ agrees with the covariant calculation in Feynman gauge.

3.5 Quark mass and wavefunction renormalization

For the energy correction to a state, the final state is identical to the initial state and hence to second order we have,

$$\delta p_i^- = \sum_n \frac{\mid \langle i \mid V_s(0) \mid n \rangle \mid^2}{p_i^- - p_n^- + i\epsilon}. \tag{3.23}$$

To one loop order, consider the following correction to the quark energy (see Fig. 3.d).

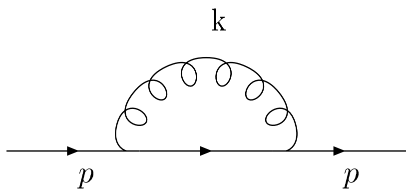

Fig. 3.d

Following the rules, we get,

$$\begin{aligned}
\delta p^- \quad &= g^2 T^a T^a \sqrt{p^+}\sqrt{p^+} \int \frac{dk_1^+ d^2k_1^\perp}{2(2\pi)^3 k_1^+}\theta(k_1^+) \int \frac{dk_2^+ d^2k_2^\perp}{2(2\pi)^3 k_2^+}\theta(k_2^+) \\
&\sqrt{k_1^+}\sqrt{k_2^+}\ 2(2\pi)^3\delta^3(P-k_1-k_2)\ 2(2\pi)^3\delta^3(P-k_1-k_2) \\
&\sum_{\lambda_1 s_2} \chi_{s_2}^\dagger \Big[\frac{2k_1^\perp}{k_1^+} - \frac{\hat\sigma^\perp.k_2^\perp - im}{k_2^+}\hat\sigma^\perp - \hat\sigma^\perp\frac{\hat\sigma^\perp.p^\perp + im}{p^+}\Big]\chi_s \cdot (\epsilon_{\lambda_1}^\perp)^* \\
&\sum_{\lambda_1 s_2} \chi_s^\dagger \Big[\frac{2k_1^\perp}{k_1^+} - \hat\sigma^\perp\frac{\hat\sigma^\perp.k_2^\perp + im}{k_2^+} - \frac{\hat\sigma^\perp.p^\perp - im}{p^+}\hat\sigma^\perp\Big]\chi_{s_2} \cdot (\epsilon_{\lambda_1}^\perp) \\
&\frac{1}{p^- - k_1^- - k_2^-}.
\end{aligned} \tag{3.24}$$

We introduce the boost invariant internal relative momenta

$$x_i = \frac{k_i^+}{p^+}, \quad \kappa_i^\perp = k^\perp - \frac{k_i{}^+}{p^+}p_i^\perp, \tag{3.25}$$

with $\sum_i x_i = 1$ and $\sum_i \kappa_i^\perp = 0$. For simplicity we further put $x_1 = x$ and $\kappa_1^\perp = \kappa^\perp$. After some algebra we find that both the numerator and denominator are independent of $p^\perp$ and further simplifications lead to

$$\frac{\delta p^-}{2(2\pi)^3 p^+ \delta^3(0)} \quad = \frac{1}{p^+}(-g^2)C_f \int \frac{dx d^2k^\perp}{2(2\pi)^3}\frac{1}{1-x}\frac{\Big[[4\frac{1}{x^2} - 4\frac{1}{x} + 2](k^\perp)^2 + 2m^2x^2\Big]}{(k^\perp)^2 + m^2x^2}. \tag{3.26}$$

We have used $(T^aT^a)_{\beta\alpha} = C_f \delta_{\beta\alpha}$ where $C_f = \frac{N^2-1}{2N}$ for $SU(N)$.

From quantum mechanical perturbation theory, the second order correction to the wavefunction is given by

$$Z_2 = 1 - \sum_n{}' \frac{\mid \langle i \mid V_s(0) \mid n \rangle \mid^2}{(p_i^- - p_n^-)^2}. \tag{3.27}$$

Thus quark wavefunction renormalization correction to second order is given by

$$\begin{aligned} Z_2^{(2)} &= (-g^2) C_f \int \frac{dx d^2 k^\perp}{2(2\pi)^3} x(1-x) \frac{1}{1-x} \frac{\left[[4\frac{1}{x^2} - 4\frac{1}{x} + 2](k^\perp)^2 + 2m^2x^2\right]}{\{(k^\perp)^2 + m^2x^2\}^2} \\ &= \frac{g^2}{8\pi^2} C_f \left(2\ ln\ \epsilon + \frac{3}{2}\right) ln \frac{\Lambda^2}{\mu^2}. \end{aligned} \tag{3.28}$$

3.6 Vertex correction: A history and motivation

The study of asymptotic freedom in non-abelian gauge theory has a long history[1]. The celebrated calculations[2, 3, 4] were done in covariant gauges. In covariant gauges, loop contribution from Faddeev-Popov ghosts are a necessary ingredient to ensure the correct coefficient which determines the approach to asymptotic freedom. In Coulomb gauge, ghosts are not involved in the lowest order and asymptotic freedom arises from a diagram involving both transverse and Coulomb gluons [5, 6, 7, 8]. In axial gauge $A^3 = 0$ (which has some similarities to light-front gauge $A^+ = 0$), Faddeev-Popov ghosts are decoupled to all orders but the gauge propagator contains severe $\frac{1}{q.\eta}$ and $\frac{1}{(q.\eta)^2}$ singularities where q is the gauge boson momentum and η is the space-like vector characterising the axial gauge. With the prescription for the double pole which is *defined* to be obtained by the differentiation of the principal value prescription for the single pole, the correct value is obtained for the ultraviolet divergent part of the gluon wavefunction renormalization constant [6, 9]. As noted by Frenkel and Taylor[6] the crucial fact is that the gluon spectral function which is formally positive receives a negative contribution because of the $\frac{1}{(q_3)^2}$ gauge singularity in $A^3 = 0$ gauge and in turn causes antiscreening.

Previous calculations in light-front gauge can be classified into four different categories. Earliest calculation by Thorn[10] was done for the pure Yang-Mills theory in the context of four-dimensional loop integrals with non-covariant regularization (k^- integration first and seperate cutoffs for k^+ and $k^\perp$). Thorn studied the four-gluon vertex for the kinematic choice of zero external transverse momenta and arrived at the well-known result for the running coupling constant. As a part of developing calculational techniques to study the evolution of hadronic structure functions, Curci, Furmanski, and Petronzio[11] studied radiative corrections to quark-gluon vertex in $A^+ = 0$ gauge. These authors considered massless quarks and employed dimensional regularization as the ultraviolet regulator and principal value prescription for $\frac{1}{k^+}$ gauge singularity. They also utilized an "infinite-momentum parametrization" of the momenta[12]. As a consequence of principal value prescription, various renormalization "constants" depend on longitudinal momenta. In addition, various renormalization constants contain product of ultraviolet regulator and principal value regulator (the so-called mixing problem). This mixing is an inevitable consequence of Hamiltonian field theory with only physical degrees of freedom as emphasized by Thorn who first observed this effect. In the calculation of Curci *et. al.*, however, when all the renormalization constants are collected to compute the radiative correction to the coupling constants, the unwanted products all cancel and one recovers the well-known running coupling constant. There exist also calculations which utilize four-dimensional integrals and choose Mandelstam-Leibbrandt prescription[13, 14] for the gauge singularity and dimensional regularization for the ultraviolet divergence. In this context there have been formulations where a) the unphysical gauge degrees of freedom are explicitly eliminated in the Lagrangian using the constraint equations (for the case of pure Yang-Mills theory see [15, 16]) and b) the unphysical gauge degrees of freedom are kept[17]. In the former case, because of gauge fixing, one can no longer verify Slavnov-Taylor identities but the loop calculations are very simple and renormalizability is quite transparent. In the latter case, since the residual gauge freedoms are kept, one can explicitly verify Slavanov-Taylor identities even though loop calculations are very complicated and the discussion of renormalizability is quite intricate. For an excellent discussion of the two formalisms for Yang-Mills theory see Ref. [16]. The Mandelstam-Leibbrandt (M-L) prescription which is essential for the success of these approaches makes Wick rotation and Euclidean power counting possible for four-dimensional loop integrals in Feynman perturbation theory. The M-L prescription as such cannot be applied to Hamiltonian light front perturbation theory[18]. In old-fashioned light-front perturbation theory, one has to deal with three-dimensional non-covariant integrals and further the light-front power counting is very diffrent from equal-time power counting[19]. Hence there is no a priori reason to abandon principal value prescription in old-fashioned light-front perturbation theory. One should study in detail the criteria for renormalizability in the Hamiltonian framework. As a starting point one should investigate the cancellation of gauge singularities in physically relevent quantities. The study of the renormalization of quark-gluon coupling in QCD in lowest order offers this opportunity.

A further motivation to investigate the running of the coupling constant in light-front gauge in old-fashioned perturbation theory arises from the study of high-energy inclusive and exclusive reactions in QCD. As is well-known (see for example, Ref. [20, 11, 21]) in order to have a successfull partonic interpretation of these physical processes it is essential to work in gauges where the gluon has only physical degrees of freedom. Furthermore, as Drell, Levy and Yan[22] and Bjorken, Kogut and Soper[23] have argued, old-fashioned perturbation theory and triviality of vacuum are essential ingredients for a probabilistic interpretation of parton densities. In order to develop a perturbative approach to exclusive reactions in QCD, as Brodsky and Lepage[24] have emphasized, the formalism of old-fashioned perturbation theory and light-front quantization are very convenient tools. Thus a study of the origin of antiscreening in light-front QCD utilizing old-fashioned perturbation theory in the Hamiltonian context (which employs only physical degrees of freedom) becomes extremely relevant for the systematic calculation of physical processes in high-energy QCD.

Another motivation to study the renormalization of coupling constant in light-front QCD comes from our ultimate objective of studying bound states in QCD. The relativistic bound state equations require regularization and renormalization. The renormalization procedure requires us to take the cutoff to be much larger than the mass scales of the bound states. In theories that lack asymptotic freedom, larger cutoffs imply small renormalized couplings and weak effective couplings in the low-momentum region. This results in almost nonrelativistic bound states or even no bound states (triviality problem). An example of this phenomena is provided in Ref. [25]. A theory that possess asymptotic freedom may help us to perform renormalization in a more meaningful manner by allowing us to choose cutoffs to be much larger than bound state mass scales. Furthermore, in such a theory the effective coupling grows at small momenta irrespective of the value of the renormalized coupling and the possibility arises for building strongly bound states irrespective of weak renormalized coupling. However, just the knowledge that the theory possess asymptotic freedom is no gaurantee that renormalization may be carried out in a simple manner in a bound state calculation. This is because in practice, we have to truncate the Fock space in order to make the numerical problem tractable on a computer. Since Feynman diagrams hide multiparticle intermediate states behind covariant propagators, what minimal Fock space states are to be included in order to overcome the triviality problem is obscure in the context of covariant calculations. This issue is naturally resolved in the old-fashioned Hamiltonian perturbation theory calculations. In our presentation we follow the calculations presented in Refs. [26, 27, 28].

3.6.1 Quark-gluon vertex in light-front QCD

The canonical light-front Hamiltonian contains several different three-point and four-point interactions and a priori there is no reason to assume that the strengths of various interactions will renormalize in the same manner. In principle one should study the evolution of the strengths of all the interactions that appear in the Hamiltonian. At present, however, we do not undertake this ambitious program. Instead we study one particular quark-gluon vertex, the one arising from the three-point interaction. We investigate radiative corrections to this vertex for different choices of external momenta.

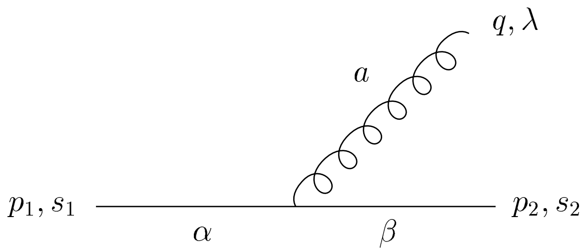

Fig. 3.1

The lowest order three-point quark-gluon interaction matrix element (Fig. 3.1) in the two-component formalism of Ref. [29] is given by

$$\mathcal{M}_0 = -g\, T^a_{\beta\alpha}\, \sqrt{p_1^+ p_2^+}\, \chi^\dagger_{\lambda_2} \Big[\frac{2q^i}{q^+} - \frac{\sigma^\perp . p_2^\perp}{p_2^+} \sigma^i - \sigma^i \frac{\sigma^\perp . p_1^\perp}{p_1^+} + im (\frac{1}{p_2^+} - \frac{1}{p_1^+}) \sigma^i \Big] \chi_{\lambda_1}\, \epsilon^{i*}_\sigma . \quad (3.29)$$

For convenience of notation, in this section we denote $\hat{\sigma}^\perp$ by $\sigma^\perp$. If we set all external transverse momenta to zero, only the helicity-flip part of the matrix element survives:

$$\mathcal{M}_{02} = g\, T^a_{\beta\alpha} \sqrt{p_1^+ p_2^+} im (\frac{1}{p_1^+} - \frac{1}{p_2^+}) \chi^\dagger_{\lambda_2} \sigma^i \chi_{\lambda_1} \epsilon^{i*}_\sigma . \quad (3.30)$$

Since mass m and g appear in this vertex multiplicatively, we expect the vertex correction to be of the form

$$\delta\mathcal{M}_{02} = i\Big(m\delta g + g\delta m\Big)\, T^a_{\beta\alpha} \sqrt{p_1^+ p_2^+} (\frac{1}{p_1^+} - \frac{1}{p_2^+}) \chi^\dagger_{\lambda_2} \sigma^i \chi_{\lambda_1} \epsilon^{i*}_\sigma . \quad (3.31)$$

Thus we expect in addition to the coupling constant renormalization a "vertex mass" correction also occuring due to radiative corrections. In the following we study the radiative corrections to both the helicity flip (m dependent) and the helicity non-flip (m independent) parts of the quark-gluon vertex. We will see that the contributions of various time-ordered diagrams depend crucially on the kinematical choice of external momenta. The study of radiative corrections to $\mathcal{M}_{02}$ is especially interesting following the observation[19] that *in light-front quantization in 3+1 dimensions, chirality is the same as helicity.* $\mathcal{M}_{02}$ is the only helicity-flip interaction in the entire canonical light-front QCD Hamiltonian. The coupling constant and the quark mass enter multiplicatively in this vertex. Thus a separate identification of the "vertex mass counterterm" is necessary in order to isolate the radiative corrections to the coupling constant. Note that the mass counterterm (which preserves particle number) is quadratic in the quark mass whereas the "vertex mass counterterm" (which changes particle number) is linear in the quark mass.

3.6.2 Massless case

The canonical quark-gluon vertex in our notation is (see Fig. 3.1)

$$\mathcal{V}_1 \; = \; g\, T^a\, \sqrt{p_1^+\, p_2^+}\, \chi^\dagger_{\lambda_2} \Big[-2\frac{q^\perp}{q^+} + \sigma^\perp \frac{\sigma^\perp . p_1^\perp}{p_1^+} + \frac{\sigma^\perp . p_2^\perp}{p_2^+} \sigma^\perp + im\Big(\frac{1}{p_1^+} - \frac{1}{p_2^+}\Big) \Big]\, \chi_{\lambda_1} \cdot (\epsilon^\perp_\sigma)^* . \quad (3.32)$$

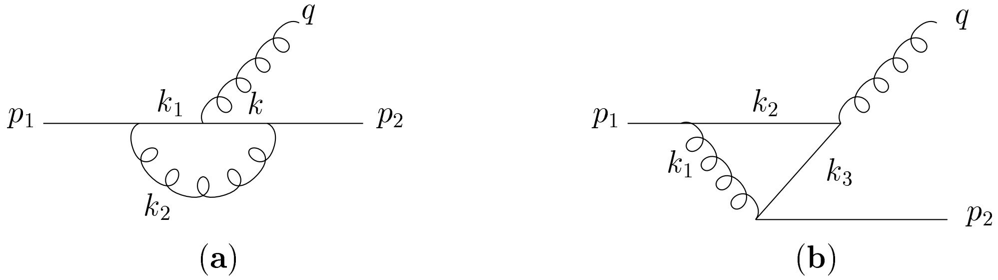

Fig. 3.2

Consider the one loop corrections to the vertex involving two quark-gluon vertices. There are two time-ordering contributions shown in Figs. 3.2(a) and 3.2(b). The contribution from Fig. 3.2(a) is

$$\begin{aligned}
\mathcal{V}_{2a} = & \frac{g^3}{2(2\pi)^3} T^b T^a T^b \sqrt{p_1^+ \, p_2^+} \int_\epsilon^{p_2^+ - \epsilon} dk^+ \int d^2k^\perp \; \theta(\Lambda - \mid k^\perp \mid)\theta(\mid k^\perp \mid) - \mu) \\
& \frac{1}{k_3^+} \frac{1}{p_1^- - k_1^- - k_3^-} \frac{1}{p_1^- - q^- - k^- - k_3^-} \\
& \sum_{\sigma_1 \sigma_2 \lambda} \chi_{\lambda_2}^\dagger \Big[-2\frac{k_3^\perp}{k_3^+} + \sigma^\perp \frac{\sigma^\perp . k^\perp}{k^+} + \frac{\sigma^\perp . p_2^\perp}{p_2^+} \sigma^\perp \Big] \chi_{\sigma_1} \cdot \epsilon_\lambda^\perp \\
& \chi_{\sigma_1}^\dagger \Big[-2\frac{q^\perp}{q^+} + \sigma^\perp \frac{\sigma^\perp . k_1^\perp}{k_1^+} + \frac{\sigma^\perp . k^\perp}{k^+} \sigma^\perp \Big] \; \chi_{\sigma_2} \cdot (\epsilon_\sigma^\perp)^* \\
& \chi_{\sigma_2}^\dagger \Big[-2\frac{k_3^\perp}{k_3^+} + \sigma^\perp \frac{\sigma^\perp . p_1^\perp}{p_1^+} + \frac{\sigma^\perp . k_1^\perp}{k_1^+} \sigma^\perp \Big] \chi_{\lambda_1} \cdot (\epsilon_\lambda^\perp)^* . \qquad (3.33)
\end{aligned}$$

Here $k_1^{(+,\perp)} = q^{(+,\perp)} + k^{(+,\perp)}$ and $k_3^{(+,\perp)} = p_2^{(+,\perp)} - k^{(+,\perp)}$. After a long and tedious calculation, we arrive at two types of divergent contributions, one containing product of logarithms and other containing a single logarithm. We have taken μ and Λ to be much larger than the external momentum scales in the problem. Divergent contributions that contain products of logarithms:

$$\begin{aligned}
\mathcal{V}_{2a}^I = & \; g \, T^a \sqrt{p_1^+ \, p_2^+} \, \chi_{\lambda_2}^\dagger \Big[-2\frac{q^\perp}{q^+} + \sigma^\perp \frac{\sigma^\perp . p_1^\perp}{p_1^+} + \frac{\sigma^\perp . p_2^\perp}{p_2^+} \sigma^\perp \Big] \chi_{\lambda_1} \cdot (\epsilon_\sigma^\perp)^* \\
& \frac{g^2}{8\pi^2} \Big(-\frac{1}{2} \, C_A \; + \; C_f \Big) \; ln\frac{\Lambda}{\mu} \; 4 \; ln\frac{p_2^+}{\epsilon} . \qquad (3.34)
\end{aligned}$$

Since the coefficient of the divergent factor is proportional to the canonical vertex, the transverse boost invariance of the above result is manifest. Divergent contributions that contain single logarithm are

$$\begin{aligned}
\mathcal{V}_{2a}^{II} = & \; g \, T^a \sqrt{p_1^+ \, p_2^+} \, \chi_{\lambda_2}^\dagger \Big[6\frac{q^\perp}{q^+} - 6\frac{p_1^\perp}{p_1^+} - \frac{\sigma^\perp . p_2^\perp}{p_1^+} \sigma^\perp + \frac{p_2^+}{p_1^+} \frac{\sigma^\perp . p_1^\perp}{p_1^+} \sigma^\perp \Big] \chi_{\lambda_1} \cdot (\epsilon_\sigma^\perp)^* \\
& \frac{g^2}{8\pi^2} \Big(-\frac{1}{2} \, C_A \; + \; C_f \Big) \; ln\frac{\Lambda}{\mu} . \qquad (3.35)
\end{aligned}$$

In this case the coefficient of the divergent factor involving transverse momenta is not proportional to the canonical vertex. However, in terms of the internal momenta, the quantity inside the square bracket can be rewritten as

$$\begin{aligned}
& \Big[6\frac{q^\perp}{q^+} - 6\frac{p_1^\perp}{p_1^+} - \frac{\sigma^\perp . p_2^\perp}{p_1^+} \sigma^\perp + \frac{p_2^+}{p_1^+} \frac{\sigma^\perp . p_1^\perp}{p_1^+} \sigma^\perp \Big] \\
& \qquad = -\frac{1}{P^+} \Big[\frac{6\kappa_1^\perp}{1-x} + \sigma^\perp . \kappa_1^\perp \sigma^\perp \Big], \qquad (3.36)
\end{aligned}$$

which satisfies the constraint from Galilean invariance.

Contribution from Fig. 3.2(b) is

$$
\begin{aligned}
\mathcal{V}_{2b} \;=\; & (-)\,\frac{g^3}{2(2\pi)^3}\; T^b T^a T^b \sqrt{p_1^+\; p_2^+}\; \int_{\epsilon}^{q^+-\epsilon} dk_2^+ \int d^2 k_2^{\perp} \\
& \theta(\Lambda - \mid k^{\perp} \mid)\; \frac{1}{p_1^+ - k_2^+}\; \frac{1}{p_1^- - k_1^- - k_2^-} \\
& \frac{1}{p_1^- - k_2^- - k_3^- - p_2^-} \sum_{\sigma_1 \sigma_2 \lambda} \chi_{\lambda_2}^{\dagger} \Big[-2\frac{k_1^{\perp}}{k_1^+} + \sigma^{\perp}\frac{\sigma^{\perp}.k_3^{\perp}}{k_3^+} + \frac{\sigma^{\perp}.p_2^{\perp}}{p_2^+}\sigma^{\perp}\Big]\, \chi_{\sigma_1}\, .\, \epsilon_{\lambda}^{\perp} \\
& \chi_{\sigma_1}^{\dagger} \Big[-2\frac{q^{\perp}}{q^+} + \sigma^{\perp}\frac{\sigma^{\perp}.k_2^{\perp}}{k_2^+} + \frac{\sigma^{\perp}.k_3^{\perp}}{k_3^+}\sigma^{\perp}\Big]\, \chi_{\sigma_2}\, .\, (\epsilon_{\sigma}^{\perp})^* \\
& \chi_{\sigma_2}^{\dagger} \Big[-2\frac{k_1^{\perp}}{k_1^+} + \sigma^{\perp}\frac{\sigma^{\perp}.p_1^{\perp}}{p_1^+} + \frac{\sigma^{\perp}.k_2^{\perp}}{k_2^+}\sigma^{\perp}\Big]\, \chi_{\lambda_1}\, .\, (\epsilon_{\lambda}^{\perp})^* .
\end{aligned} \tag{3.37}
$$

Here $k_1^{(+,\perp)} = p_1^{(+,\perp)} - k_2^{(+,\perp)}$ and $k_3^{(+,\perp)} = q^{(+,\perp)} - k_2^{(+,\perp)}$. The overall $-ve$ sign arises from the anti symmetry property of fermionic states. Note that this $-ve$ sign is missing from Eq. (A8) of Ref.[27].

As in the previous case, explicit evaluation leads to terms containing two types of divergences. Divergent contributions that contain products of logarithms are

$$
\begin{aligned}
\mathcal{V}_{2b}^{I} \;=\; & g\; T^a \sqrt{p_1^+}\sqrt{p_2^+}\; \chi_{\lambda_2}^{\dagger} \Big[-2\frac{q^{\perp}}{q^+} + \sigma^{\perp}\frac{\sigma^{\perp}.p_1^{\perp}}{p_1^+} + \frac{\sigma^{\perp}.p_2^{\perp}}{p_2^+}\sigma^{\perp}\Big]\, \chi_{\lambda_1}\, .\, (\epsilon_{\sigma}^{\perp})^* \\
& \frac{g^2}{8\pi^2}\Big(-\frac{1}{2}\; C_A \;+\; C_f \Big)\; ln\frac{\Lambda}{\mu}\; 2\; ln\frac{p_1^+}{p_2^+}.
\end{aligned} \tag{3.38}
$$

Again, the transverse boost invariance of this result is manifest since the contribution is proportional to the canonical vertex. Divergent contributions that contain single logarithm are

$$
\begin{aligned}
\mathcal{V}_{2b}^{II} \;=\; & (-)\; g\; T^a \sqrt{p_1^+\; p_2^+}\; \chi_{\lambda_2}^{\dagger} \Big[3\sigma^{\perp}\frac{\sigma^{\perp}.p_1^{\perp}}{p_1^+} + 3\frac{\sigma^{\perp}.p_2^{\perp}}{p_2^+}\sigma^{\perp} \\
& -6\frac{p_1^{\perp}}{p_1^+} - \frac{\sigma^{\perp}.p_2^{\perp}}{p_1^+}\sigma^{\perp} + \frac{p_2^+}{p_1^+}\frac{\sigma^{\perp}.p_1^{\perp}}{p_1^+}\sigma^{\perp}\Big]\, \chi_{\lambda_1}\, .\, (\epsilon_{\sigma}^{\perp})^* \\
& \frac{g^2}{8\pi^2}\Big(-\frac{1}{2}\; C_A \;+\; C_f \Big)\; ln\frac{\Lambda}{\mu}.
\end{aligned} \tag{3.39}
$$

The transverse boost symmetry of the terms inside the square bracket is not manifest but becomes explicit once we express the result in terms of the internal momenta. Alternatively, by subtracting and adding the term $-6\frac{q^{\perp}}{q^+}$ to these terms we can rewrite the terms inside the square bracket as the canonical term plus the terms contained in the square bracket in eq.(3.35) which again shows the boost invariance of the result in eq.(3.39).

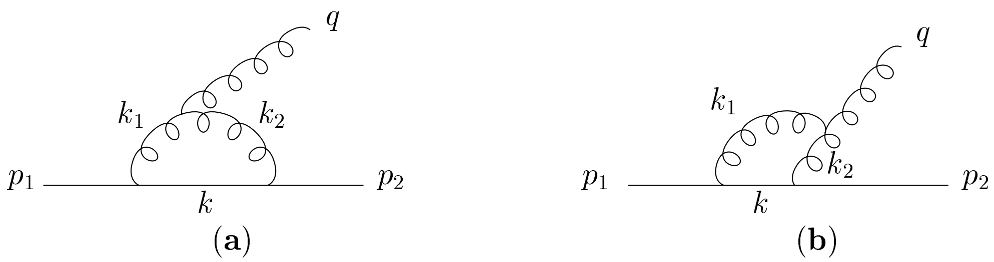

Fig. 3.3

Consider, next, the one loop contributions to the quark-gluon vertex involving one quark-gluon vertex and one three gluon vertex. There are two time ordering contributions shown in Figs. 3.3(a) and 3.3(b). The contribution from Fig. 3.3(a) is

$$
\begin{aligned}
\mathcal{V}_{3a} \;=\;\; & \frac{g^3}{2(2\pi)^3}\,(-if^{abc}T^bT^c)\,\sqrt{p_1^+\,p_2^+}\,\int_\epsilon^{p_2^+-\epsilon} dk^+\,\int d^2k^\perp \\
& \theta(\Lambda-\mid k^\perp\mid)\,\frac{1}{k_1^+}\,\frac{1}{k_2^+}\,\frac{1}{p_1^- - k_1^- - k^-} \\
& \frac{1}{p_1^- - q^- - k_2^- - k^-}\,\sum_{\sigma_1,\rho_1,\rho_2}\chi^\dagger_{\lambda_2}\Big[-2\frac{k_2^\perp}{k_2^+}+\sigma^\perp\frac{\sigma^\perp.k^\perp}{k^+}+\frac{\sigma^\perp.p_2^\perp}{p_2^+}\sigma^\perp\Big]\,\chi_{\sigma_1}\,.\,\epsilon^\perp_{\rho_2} \\
& \chi^\dagger_{\sigma_1}\Big[-2\frac{k_1^\perp}{k_1^+}+\sigma^\perp\frac{\sigma^\perp.p_1^\perp}{p_1^+}+\frac{\sigma^\perp.k^\perp}{k^+}\sigma^\perp\Big]\,\chi_{\lambda_1}\,.\,(\epsilon^\perp_{\rho_1})^*\epsilon^j_{\rho_1}\,(\epsilon^i_\sigma)^*\,(\epsilon^l_{\rho_2})^* \\
& \Bigg[\Big[(k_1^i+k_2^i)-\frac{q^i}{q^+}(k_1^++k_2^+)\Big]\delta_{lj}-\Big[(k_1^l+q^l)-\frac{k_2^l}{k_2^+}(k_1^++q^+)\Big]\delta_{ij} \\
& \quad +\Big[(q^j-k_2^j)-\frac{k_1^j}{k_1^+}(q^+-k_2^+)\Big]\delta_{il}\Bigg].
\end{aligned}
\tag{3.40}
$$

Here $k_1^{(+,\perp)} = p_1^{(+,\perp)} - k^{(+,\perp)}$ and $k_2^{(+,\perp)} = p_2^{(+,\perp)} - k^{(+,\perp)}$. Divergent contributions that contain products of logarithms are

$$
\begin{aligned}
\mathcal{V}^I_{3a} \;=\;\; & g\,T^a\,\sqrt{p_1^+\,p_2^+}\,\chi^\dagger_{\lambda_2}\Big[-2\frac{q^\perp}{q^+}+\sigma^\perp\frac{\sigma^\perp.p_1^\perp}{p_1^+}+\frac{\sigma^\perp.p_2^\perp}{p_2^+}\sigma^\perp\Big]\,\chi_{\lambda_1}\,.\,(\epsilon^\perp_\sigma)^* \\
& \frac{g^2}{8\pi^2}\,\frac{1}{2}\,C_A\,ln\frac{\Lambda}{\mu}\,2\,ln\frac{p_1^+p_2^+}{q^+\epsilon}.
\end{aligned}
\tag{3.41}
$$

The boost invariance of this result is again clear. Divergent contributions that contain single logarithm are

$$
\begin{aligned}
\mathcal{V}^{II}_{3a} \;=\;\; & g\,T^a\,\sqrt{p_1^+\,p_2^+}\,\chi^\dagger_{\lambda_2}\Big[6\frac{q^\perp}{q^+}-6\frac{p_1^\perp}{p_1^+}+\frac{\sigma^\perp.p_2^\perp}{p_1^+}\sigma^\perp-\frac{p_2^+}{p_1^+}\frac{\sigma^\perp.p_1^\perp}{p_1^+}\sigma^\perp\Big]\,\chi_{\lambda_1}\,.\,(\epsilon^\perp_\sigma)^* \\
& \frac{g^2}{8\pi^2}\,\frac{1}{2}\,C_A\,ln\frac{\Lambda}{\mu}.
\end{aligned}
\tag{3.42}
$$

Expressing the terms inside the square bracket in terms of the internal momenta we get $-\frac{1}{P^+}\Big[\frac{6\kappa_1^\perp}{1-x}-\sigma^\perp.\kappa_1^\perp\sigma^\perp\Big]$ which makes boost invariance explicit.

The contribution from Fig. 3.3(b) is

$$\mathcal{V}_{3b} = \frac{g^3}{2(2\pi)^3}(-if^{abc}T^bT^c)\sqrt{p_1^+\, p_2^+}$$
$$\int_\epsilon^{q^+-\epsilon} dk_1^+ \int d^2k_1^\perp\, \theta(\Lambda - \mid k^\perp \mid)\frac{1}{k_1^+}\,\frac{1}{k_2^+}\,\frac{1}{p_1^- - k_1^- - k^-}$$
$$\frac{1}{p_1^- - k_1^- - k_2^- - p_2^-}\sum_{\sigma_1\rho_1\rho_2}\chi_{\lambda_2}^\dagger\Big[-2\frac{k_2^\perp}{k_2^+} + \sigma^\perp\frac{\sigma^\perp.k^\perp}{k^+} + \frac{\sigma^\perp.p_2^\perp}{p_2^+}\sigma^\perp\Big]\,\chi_{\sigma_1}\,.\,(\epsilon_{\rho_2}^\perp)^*$$
$$\chi_{\sigma_1}^\dagger\Big[-2\frac{k_1^\perp}{k_1^+} + \sigma^\perp\frac{\sigma^\perp.p_1^\perp}{p_1^+} + \frac{\sigma^\perp.k^\perp}{k^+}\sigma^\perp\Big]\,\chi_{\lambda_1}\,.\,(\epsilon_{\rho_1}^\perp)^*$$
$$\epsilon_{\rho_1}^j\,(\epsilon_\sigma^i)^*\,\epsilon_{\rho_2}^l\,\Bigg[\Big[(k_1^i - k_2^i) - \frac{q^i}{q^+}(k_1^+ - k_2^+)\Big]\delta_{lj} - \Big[(k_1^l + q^l) - \frac{k_2^l}{k_2^+}(k_1^+ + q^+)\Big]\delta_{ij}$$
$$+\Big[(q^j + k_2^j) - \frac{k_1^j}{k_1^+}(q^+ + k_2^+)\Big]\delta_{il}\Bigg]. \tag{3.43}$$

Here $k^{(+,\perp)} = p_1^{(+,\perp)} - k_1^{(+,\perp)}$ and $k_2^{(+,\perp)} = q^{(+,\perp)} - k_1^{(+,\perp)}$.

Divergent contributions that contain products of logarithms are

$$\mathcal{V}_{3b}^I = g\,T^a\sqrt{p_1^+\,p_2^+}\,\chi_{\lambda_2}^\dagger\Big[-2\frac{q^\perp}{q^+} + \sigma^\perp\frac{\sigma^\perp.p_1^\perp}{p_1^+} + \frac{\sigma^\perp.p_2^\perp}{p_2^+}\sigma^\perp\Big]\,\chi_{\lambda_1}\,.\,(\epsilon_\sigma^\perp)^*$$
$$\frac{g^2}{8\pi^2}\,\frac{1}{2}C_A\,ln\frac{\Lambda}{\mu}\,6\,ln\frac{q^+}{\epsilon} \tag{3.44}$$

which is manifestly boost invariant. Divergent contributions that contain single logarithm are

$$\mathcal{V}_{3b}^{II} = g\,T^a\sqrt{p_1^+}\,\sqrt{p_2^+}\,\chi_{\lambda_2}^\dagger\Big[-3\sigma^\perp\frac{\sigma^\perp.p_1^\perp}{p_1^+} - 3\frac{\sigma^\perp.p_2^\perp}{p_2^+}\sigma^\perp$$
$$+6\frac{p_1^\perp}{p_1^+} + \frac{p_2^+}{p_1^+}\,\frac{\sigma^\perp.p_1^\perp}{p_1^+}\sigma^\perp - \frac{\sigma^\perp.p_2^\perp}{p_1^+}\sigma^\perp\Big]\,\chi_{\lambda_1}\,.\,(\epsilon_\sigma^\perp)^*\frac{g^2}{8\pi^2}\,\frac{1}{2}\,C_A\,ln\frac{\Lambda}{\mu}. \tag{3.45}$$

Comparison with Eq. (3.39) again makes the boost invariance of this answer explicit.

Coupling constant renormalization

For the sake of completeness, we present here the results for the other diagrams which are relevant for the coupling constant renormalization. We also calculate the β-function which exactly matches with the well known results and therefore extends the results arrived at in the Ref.([5]), to the *most general kinematics* in the two-component formalism.

The sum of divergent contributions from Figs. 3.2(a) and 3.2(d) is

$$\mathcal{V}_2 = gT^a\sqrt{p_1^+\,p_2^+}\,\chi_{\lambda_2}^\dagger\Big[-2\frac{q^\perp}{q^+} + \sigma^\perp\frac{\sigma^\perp.p_1^\perp}{p_1^+} + \frac{\sigma^\perp.p_2^\perp}{p_2^+}\sigma^\perp\Big]\,\chi_{\lambda_1}\,.\,(\epsilon_\sigma^\perp)^*$$
$$\frac{g^2}{8\pi^2}\Big(-\frac{1}{2}\,C_A\,+\,C_f\Big)\,ln\frac{\Lambda}{\mu}\,\Big(2\,ln\frac{p_1^+p_2^+}{\epsilon^2} - 3\Big), \tag{3.46}$$

where we observe the emergence of the canonical vertex structure.

The sum of divergent contributions from Figs. 3.3(a) and 3.3(b) is

$$\mathcal{V}_3 = g\ T^a\ \sqrt{p_1^+}\ \sqrt{p_2^+}\ \chi^\dagger_{\lambda_2}\ \Big[-2\frac{q^\perp}{q^+}+\sigma^\perp\frac{\sigma^\perp.p_1^\perp}{p_1^+}+\frac{\sigma^\perp.p_2^\perp}{p_2^+}\sigma^\perp\Big]\ \chi_{\lambda_1}\ .\ (\epsilon_\sigma^\perp)^* \\ \frac{g^2}{8\pi^2}\frac{1}{2}\ C_A\ ln\frac{\Lambda}{\mu}\ \Big(2\ ln\frac{p_1^+p_2^+}{\epsilon^2}\ +\ 4\ ln\frac{q^+}{\epsilon}\ -\ 3\Big), \tag{3.47}$$

where we again observe the emergence of the canonical vertex.

The diagrams in Figs. 3.4(a), 3.4(b), 3.5(a) and 3.5(b) correspond to the renormalization of the external quark and gluon legs that are connected to the vertex. Their contributions are given below.

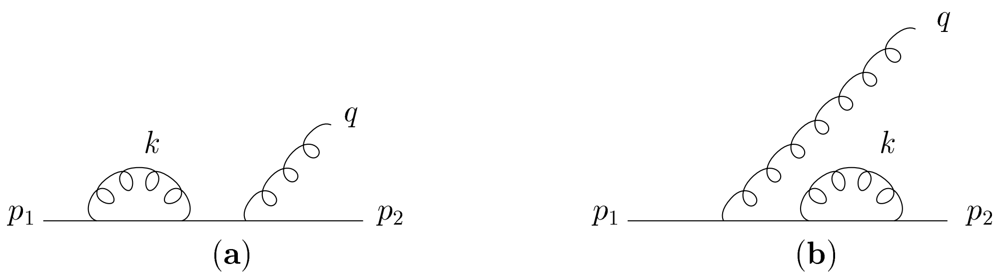

Fig. 3.4

$$\mathcal{V}_{4a} = g\ T^a\ \sqrt{p_1^+p_2^+}\ \chi^\dagger_{\lambda_2}\ \Big[-2\frac{q^\perp}{q^+}+\sigma^\perp\frac{\sigma^\perp.p_1^\perp}{p_1^+}+\frac{\sigma^\perp.p_2^\perp}{p_2^+}\sigma^\perp\Big]\ \chi_{\lambda_1}\ .\ (\epsilon_\sigma^\perp)^* \\ \frac{g^2}{4\pi^2}\ C_f\ ln\frac{\Lambda}{\mu}\ \Big(\frac{3}{2}-2\ ln\frac{p_1^+}{\epsilon}\Big), \tag{3.48}$$

$$\mathcal{V}_{4b} = g\ T^a\ \sqrt{p_1^+p_2^+}\ \chi^\dagger_{\lambda_2}\ \Big[-2\frac{q^\perp}{q^+}+\sigma^\perp\frac{\sigma^\perp.p_1^\perp}{p_1^+}+\frac{\sigma^\perp.p_2^\perp}{p_2^+}\sigma^\perp\Big]\ \chi_{\lambda_1}\ .\ (\epsilon_\sigma^\perp)^* \\ \frac{g^2}{4\pi^2}\ C_f\ ln\frac{\Lambda}{\mu}\ \Big(\frac{3}{2}-2\ ln\frac{p_2^+}{\epsilon}\Big), \tag{3.49}$$

$$\mathcal{V}_{5a} = -g\ T^a\ \sqrt{p_1^+p_2^+}\ \chi^\dagger_{\lambda_2}\ \Big[-2\frac{q^\perp}{q^+}+\sigma^\perp\frac{\sigma^\perp.p_1^\perp}{p_1^+}+\frac{\sigma^\perp.p_2^\perp}{p_2^+}\sigma^\perp\Big]\ \chi_{\lambda_1}\ .\ (\epsilon_\sigma^\perp)^* \\ \frac{g^2}{8\pi^2}\frac{4}{3}\ N_fT_f\ ln\frac{\Lambda}{\mu}. \tag{3.50}$$

$$\mathcal{V}_{5b} = g\ T^a\ \sqrt{p_1^+p_2^+}\ \chi^\dagger_{\lambda_2}\ \Big[-2\frac{q^\perp}{q^+}+\sigma^\perp\frac{\sigma^\perp.p_1^\perp}{p_1^+}+\frac{\sigma^\perp.p_2^\perp}{p_2^+}\sigma^\perp\Big]\ \chi_{\lambda_1}\ .\ (\epsilon_\sigma^\perp)^* \\ \frac{g^2}{8\pi^2}\ C_A\ ln\frac{\Lambda}{\mu}\ \Big(\frac{11}{3}-4\ ln\frac{q^+}{\epsilon}\Big), \tag{3.51}$$

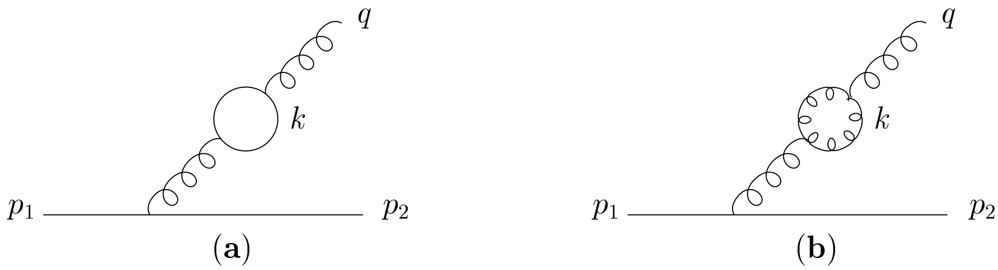

Fig. 3.5

This is not really the end of the story. There are a host of diagrams that involve either an instantaneous fermion or an instantaneous gluon (see Figs. 3.6 - 3.9). Fortunately all of them are proportional to the quark mass and vanish when the quark mass is zero. Their contributions to the renormalization of the helicity-flip vertex is considered in the next section.

Now, to evaluate the contributions to the coupling constant, we have to multiply $\mathcal{V}_2$ and $\mathcal{V}_4$ with $\frac{1}{2}$ in order to take into account the proper correction due to the renormalization of initial and final states [30]. Thus adding the contributions we get,

$$\begin{aligned}\delta\mathcal{V}_1 = &\quad (\frac{1}{2}\mathcal{V}_4 + \frac{1}{2}\mathcal{V}_5 + \mathcal{V}_2 + \mathcal{V}_3) \\ = &\quad g\ T^a\ \sqrt{p_1^+ p_2^+}\ \chi^\dagger_{\lambda_2}\ \Big[-2\frac{q^\perp}{q^+} + \sigma^\perp \frac{\sigma^\perp . p_1^\perp}{p_1^+} + \frac{\sigma^\perp . p_2^\perp}{p_2^+}\sigma^\perp \Big]\ \chi_{\lambda_1}\ .\ (\epsilon_\sigma^\perp)^* \\ &\quad \frac{g^2}{8\pi^2}\Big(\frac{11}{6}C_A - \frac{2}{3}N_f T_f\Big)\ ln\frac{\Lambda}{\mu} \end{aligned} \tag{3.52}$$

Note that all the mixed divergences cancel. The correction to the coupling constant is given by

$$g_R\ =\ g(1+\delta g)\ =\ g\Big[\ 1 + \frac{g^2}{8\pi^2}\Big(\frac{11}{6}C_A - \frac{2}{3}N_f T_f\Big) ln\frac{\Lambda}{\mu}\ \Big]. \tag{3.53}$$

We compute the β-function as

$$\begin{aligned}\beta(g) &= -\ \frac{\partial g_R}{\partial ln\Lambda} \\ &= -\ \frac{g^3}{16\pi^2}\Big(\frac{11}{3}C_A - \frac{4}{3}N_f T_f\Big),\end{aligned} \tag{3.54}$$

which is well known result to the one-loop order.

3.6.3 Renormalization of helicity flip vertex

In this section we present the results for the lowest order radiative corrections to the strength of the helicity-flip matrix element in light-front QCD using the old-fashioned perturbation theory rules. We present the results for each time ordered diagram seperately in order to exhibit the contribution from distinct intermediate Fock-space states.

The contribution from Fig. 3.2(a) is

$$\begin{aligned}
\mathcal{M}_{2a} = \quad & imgT^a_{\beta\alpha}\sqrt{p_1^+p_2^+}\chi^\dagger_{\lambda_2}\sigma^\perp.(\epsilon^\perp_\sigma)^*\chi_{\lambda_1} \\
& \times 4(-\frac{1}{2}C_A + C_f)(-)\frac{g^2}{2(2\pi)^3}\frac{1}{p_1^+}\frac{1}{p_2^+}\int\frac{d^2k^\perp}{(k^\perp)^2} \\
& \int_0^{p_2^+} dk^+[\frac{q^+}{p_2^+ - k^+} - \frac{k^+}{2p_1^+} + \frac{(k^+ + q^+)}{2p_2^+}] \\
& = imgT^a_{\beta\alpha}\sqrt{p_1^+p_2^+}\chi^\dagger_{\lambda_2}\sigma^\perp.(\epsilon^\perp_\sigma)^*\chi_{\lambda_1} \\
& \times(-\frac{1}{2}C_A + C_f)\frac{g^2}{2\pi^2}(-(\frac{1}{p_1^+} - \frac{1}{p_2^+})ln\frac{\epsilon}{p_2^+} + \frac{1}{4p_1^+} - \frac{1}{2p_2^+} + \frac{p_2^+}{4(p_1^+)^2})\ln\frac{\Lambda}{\mu}.
\end{aligned} \tag{3.55}$$

The contribution from Fig. 3.2(b) is

$$\begin{aligned}
\mathcal{M}_{2b} = \quad & imgT^a_{\beta\alpha}\sqrt{p_1^+p_2^+}\chi^\dagger_{\lambda_2}\sigma^\perp.(\epsilon^\perp_\sigma)^*\chi_{\lambda_1}(-\frac{1}{2}C_A + C_f)4\frac{1}{p_1^+}\frac{1}{q^+}(-)\frac{g^2}{2(2\pi)^3}\int\frac{d^2k^\perp}{(k^\perp)^2} \\
& \int_0^{q^+} dk^+\Big[\frac{q^+k^+}{(p_1^+ - k^+)^2} + \frac{1}{2p_1^+}\frac{k^+(q^+ - k^+)}{(p_1^+ - k^+)} + \frac{1}{2p_2^+}\frac{(k^+)^2}{(p_1^+ - k^+)}\Big] \\
& = imgT^a_{\beta\alpha}\sqrt{p_1^+p_2^+}\chi^\dagger_{\lambda_2}\sigma^\perp.(\epsilon^\perp_\sigma)^*\chi_{\lambda_1} \\
& (-\frac{1}{2}C_A + C_f)\frac{g^2}{2\pi^2}(\frac{1}{2}(\frac{1}{p_1^+} - \frac{1}{p_2^+})ln\frac{p_1^+}{p_2^+} + \frac{1}{2p_1^+} - \frac{1}{4p_2^+} - \frac{p_2^+}{4(p_1)^2}))\ln\frac{\Lambda}{\mu}.
\end{aligned} \tag{3.56}$$

The contribution from Fig. 3.3(a) is

$$\begin{aligned}
\mathcal{M}_{3a} \quad & = imgT^a_{\beta\alpha}\sqrt{p_1^+p_2^+}\chi^\dagger_{\lambda_2}\sigma^\perp.(\epsilon^\perp_\sigma)^*\chi_{\lambda_1}\frac{1}{2}C_A\frac{1}{p_1^+}\frac{1}{p_2^+}\frac{g^2}{2(2\pi)^3}\int\frac{d^2k^\perp}{(k^\perp)^2} \\
& \int_0^{p_2^+} dk^+k^+\Big(\frac{2k^+}{p_2^+q_1^+}(1 + \frac{q^+}{q_2^+} - \frac{2q^+}{q_1^+}) - \frac{2k^+}{p_1^+q_2^+}(1 - \frac{q^+}{q_1^+} + \frac{2q^+}{q_2^+}) \\
& -\frac{2}{q_1^+}(1 + \frac{q^+}{q_2^+} - \frac{2q^+}{q_1^+}) + \frac{2}{q_2^+}(1 - \frac{q^+}{q_1^+} + \frac{2q^+}{q_2^+}) + (\frac{1}{p_2^+} - \frac{1}{p_1^+})\frac{2(q^+)^2}{q_1^+q_2^+}\Big)
\end{aligned} \tag{3.57}$$

where $q_1 = p_1 - k$ and $q_2 = p_2 - k$. Thus

$$\begin{aligned}
\mathcal{M}_{3a} \quad & = imgT^a_{\beta\alpha}\sqrt{p_1^+p_2^+}\chi^\dagger_{\lambda_2}\sigma^\perp.(\epsilon^\perp_\sigma)^*\chi_{\lambda_1} \\
& \times\frac{1}{2}C_A\frac{g^2}{8\pi^2}\Big[\frac{4(q^+)^2}{(p_1^+)^2\epsilon} - \frac{2q^+}{p_1^+p_2^+}ln\frac{p_1^+p_2^+}{q^+\epsilon} + \frac{6q^+}{(p_1^+)^2}ln\frac{p_2^+}{\epsilon} \\
& +\frac{6q^+}{(p_2^+)^2}ln\frac{p_1^+}{q^+} - \frac{12q^+}{p_1^+p_2^+} - \frac{q^+}{(p_1^+)^2}\Big]\ln\frac{\Lambda}{\mu}.
\end{aligned} \tag{3.58}$$

Here we first encounter a *linear* infrared divergence in the one loop calculation of vertex in addition to the mixing term. The contribution from Fig. 3.3(b) is

$$\mathcal{M}_{3b} \quad = imgT^a_{\beta\alpha}\sqrt{p_1^+p_2^+}\chi^\dagger_{\lambda_2}\sigma^\perp.(\epsilon^\perp_\sigma)^*\chi_{\lambda_1}\frac{1}{2}C_A\frac{1}{p_1^+}\frac{1}{q^+}\frac{g^2}{2(2\pi)^3}\int\frac{d^2k^\perp}{(k^\perp)^2}\int_0^{q^+} dk^+k^+$$

$$
\begin{aligned}
&\Big(\frac{-2(p_1^+-k^+)}{p_2^+k^+}\big(-1+\frac{q^+}{(q^+-k^+)}+\frac{2q^+}{k^+}\big)-\frac{2(p_1^+-k^+)}{p_1^+(q^+-k^+)}\big(-1+\frac{q^+}{k^+}+\frac{2q^+}{(q^+-k^+)}\big)\\
&-\frac{2}{k^+}\big(1-\frac{q^+}{(q^+-k^+)}-\frac{2q^+}{k^+}\big)-\frac{2}{(q^+-k^+)}\big(1-\frac{q^+}{k^+}-\frac{2q^+}{(q^+-k^+)}\big)\\
&\quad-\big(\frac{1}{p_2^+}-\frac{1}{p_1^+}\big)\frac{2(q^+)^2}{k^+(q^+-k^+)}\Big)\\
&= imgT^a_{\beta\alpha}\sqrt{p_1^+p_2^+}\chi^\dagger_{\lambda_2}\sigma^\perp.(\epsilon^\perp_\sigma)^*\chi_{\lambda_1}\\
&\times\frac{1}{2}C_A\frac{g^2}{8\pi^2}\Big[\frac{4(q^+)^2}{(p_1^+)^2\epsilon}-\frac{6q^+}{p_1^+p_2^+}ln\frac{q^+}{\epsilon}-\frac{6q^+}{(p_1)^2}ln\frac{q^+}{\epsilon}+\frac{3q^+}{p_1^+p_2^+}+\frac{q^+}{(p_1^+)^2}\Big]\ln\frac{\Lambda}{\mu}. \qquad (3.59)
\end{aligned}
$$

Note the presence of linear infrared divergence in this contribution.

Next we give the contributions from fermion wavefunction renormalization. The time ordered diagrams are given in Figs. 3.4(a) and 3.4(b).

The contribution from Fig. 3.4(a) is

$$
\mathcal{M}_{4a} = imgT^a_{\beta\alpha}\sqrt{p_1^+p_2^+}\big(\frac{1}{p_1^+}-\frac{1}{p_2^+}\big)\chi^\dagger_{\lambda_2}\sigma^\perp.(\epsilon^\perp_\sigma)^*\chi_{\lambda_1}(-)\frac{g^2}{4\pi^2}C_F\left(2ln\frac{p_1^+}{\epsilon}-\frac{3}{2}\right)ln\frac{\Lambda}{\mu}. \qquad (3.60)
$$

The contribution from Fig. 3.4(b) is

$$
\mathcal{M}_{4b} = imgT^a_{\beta\alpha}\sqrt{p_1^+p_2^+}\big(\frac{1}{p_1^+}-\frac{1}{p_2^+}\big)\chi^\dagger_{\lambda_2}\sigma^\perp.(\epsilon^\perp_\sigma)^*\chi_{\lambda_1}(-)\frac{g^2}{4\pi^2}C_f\left(2ln\frac{{p_2}^+}{\epsilon}-\frac{3}{2}\right)ln\frac{\Lambda}{\mu}. \qquad (3.61)
$$

The combined contribution from Fig. 3.4 is

$$
\mathcal{M}_{4} = imgT^a_{\beta\alpha}\sqrt{p_1^+p_2^+}\big(\frac{1}{p_1^+}-\frac{1}{p_2^+}\big)\chi^\dagger_{\lambda_2}\sigma^\perp.(\epsilon^\perp_\sigma)^*\chi_{\lambda_1}(-)\frac{g^2}{4\pi^2}C_f\left(2ln\frac{{p_1}^+{p_2}^+}{\epsilon^2}-3\right)ln\frac{\Lambda}{\mu}. \qquad (3.62)
$$

Next we calculate the contributions from gluon wavefunction renormalization constant. The time ordered diagrams are given in Figs. 3.5(a) and 3.5(b). The contributions from fermion-anti fermion intermediate states are given by

$$
\begin{aligned}
\mathcal{M}_{5a} = \;& imgT^a_{\beta\alpha}\sqrt{p_1^+p_2^+}\big(\frac{1}{p_1^+}-\frac{1}{p_2^+}\big)\chi^\dagger_{\lambda_2}\sigma^\perp.(\epsilon^\perp_\sigma)^*\chi_{\lambda_1}(-)2N_fT_f\frac{g^2}{2(2\pi)^3}\int\frac{d^2k^\perp}{(k^\perp)^2}\\
& \frac{1}{q^+}\int_0^{q^+}dk^+\frac{(k^+)^2+(q^+-k^+)^2}{(q^+)^2}\\
& = imgT^a_{\beta\alpha}\sqrt{p_1^+p_2^+}\frac{1}{p_1^+}-\frac{1}{p_2^+}\big)\chi^\dagger_{\lambda_2}\sigma^\perp.(\epsilon^\perp_\sigma)^*\chi_{\lambda_1}\\
& \times N_fT_f\big((-)\frac{g^2}{6\pi^2}\ln\frac{\Lambda}{\mu}. \qquad (3.63)
\end{aligned}
$$

We have assumed that there are N_f flavors of fermions.

The contributions from two-gluon intermediate states are given by

$$
\begin{aligned}
\mathcal{M}_{5b} = \quad & imgT^a_{\beta\alpha}\sqrt{p_1^+p_2^+}(\frac{1}{p_1^+}-\frac{1}{p_2^+})\chi^\dagger_{\lambda_2}\sigma^\perp.(\epsilon^\perp_\sigma)^*\chi_{\lambda_1}C_A(-)\frac{g^2}{(2\pi)^3}\int\frac{d^2k^\perp}{(k^\perp)^2} \\
& \frac{1}{q^+}\int_0^{q^+}dk^+k^+(q^+-k^+)\Big[\frac{1}{(k^+)^2}+\frac{1}{(q^+-k^+)^2}+\frac{1}{(q^+)^2}\Big] \\
& = imgT^a_{\beta\alpha}\sqrt{p_1^+p_2^+}(\frac{1}{p_1^+}-\frac{1}{p_2^+})\chi^\dagger_{\lambda_2}\sigma^\perp.(\epsilon^\perp_\sigma)^*\chi_{\lambda_1}\frac{1}{2}C_A\frac{g^2}{4\pi^2}(\frac{11}{3}-4ln\frac{q^+}{\epsilon})\ln\frac{\Lambda}{\mu}.
\end{aligned}
\tag{3.64}
$$

The two-gluon intermediate state contribution is negative as one expects from old-fashioned perturbation theory solely due to the presence of mixing term. We reiterate that this a natural feature of Hamiltonian calculation with only physical degrees of freedom.

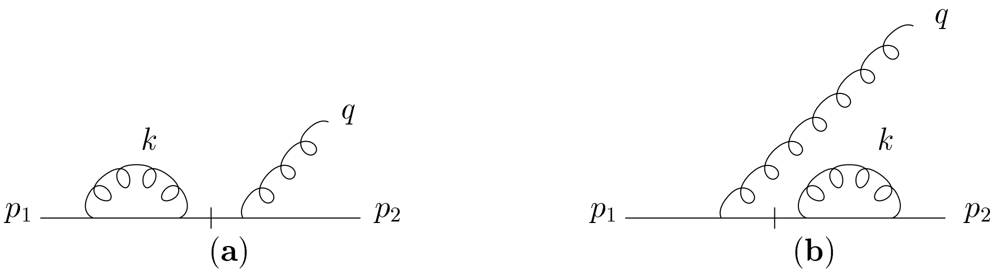

Fig. 3.6

The contribution from Fig. 3.6(a) is

$$
\begin{aligned}
\mathcal{M}_{6a} = \quad & 2imgT^a_{\beta\alpha}\sqrt{p_1^+p_2^+}\frac{1}{p_1^+}\chi^\dagger_{\lambda_2}\sigma^\perp.(\epsilon^\perp_\sigma)^*\chi_{\lambda_1}\frac{g^2}{2(2\pi)^3}C_f\int\frac{d^2k^\perp}{(k^\perp)^2}\int_0^{p_1^+}dk^+\frac{1}{p_1^+}\frac{k^+}{p_1^+} \\
& = imgT^a_{\beta\alpha}\sqrt{p_1^+p_2^+}\frac{1}{p_1^+}\chi^\dagger_{\lambda_2}\sigma^\perp.(\epsilon^\perp_\sigma)^*\chi_{\lambda_1}\frac{g^2}{8\pi^2}\,C_f\,\ln\frac{\Lambda}{\mu}.
\end{aligned}
\tag{3.65}
$$

The contribution from Fig. 3.6(b) is

$$
\begin{aligned}
\mathcal{M}_{6b} = \quad & -2imgT^a_{\beta\alpha}\sqrt{p_1^+p_2^+}\frac{1}{p_2^+}\chi^\dagger_{\lambda_2}\sigma^\perp.(\epsilon^\perp_\sigma)^*\chi_{\lambda_1}\frac{g^2}{2(2\pi)^3}\,C_f\int\frac{d^2k^\perp}{(k^\perp)^2}\int_0^{p_2^+}dk^+\frac{1}{p_2^+}\frac{k^+}{p_2^+} \\
& = -imgT^a_{\beta\alpha}\sqrt{p_1^+p_2^+}\frac{1}{p_2^+}\chi^\dagger_{\lambda_2}\sigma^\perp.(\epsilon^\perp_\sigma)^*\chi_{\lambda_1}\frac{g^2}{8\pi^2}\,C_f\,\ln\frac{\Lambda}{\mu}.
\end{aligned}
\tag{3.66}
$$

The combined contribution from Fig. 3.6 is

$$
\mathcal{M}_6 = \quad imgT^a_{\beta\alpha}\sqrt{p_1^+p_2^+}(\frac{1}{p_1^+}-\frac{1}{p_2^+})\chi^\dagger_{\lambda_2}\sigma^\perp.(\epsilon^\perp_\sigma)^*\chi_{\lambda_1}\frac{g^2}{8\pi^2}\,C_f\,\ln\frac{\Lambda}{\mu}.
\tag{3.67}
$$

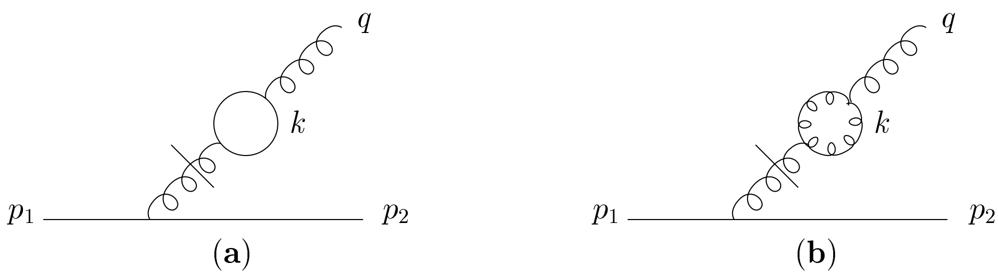

Fig. 3.7

The contributions from Fig. 3.7 are

$$\mathcal{M}_{7a} = 0. \tag{3.68}$$

$$\mathcal{M}_{7b} = 0. \tag{3.69}$$

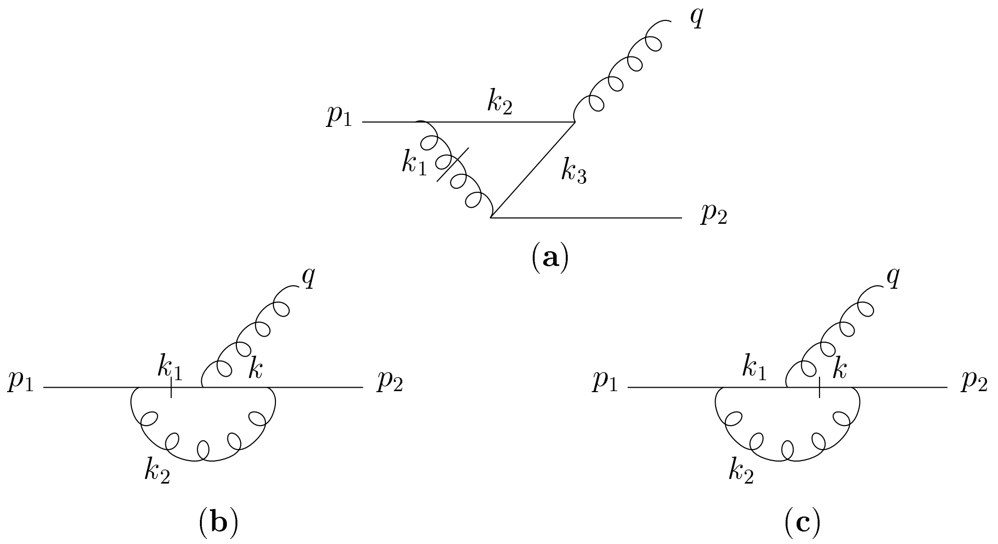

Fig. 3.8

The contribution from Fig. 3.8(a) is

$$\begin{aligned}\mathcal{M}_{8a} = \quad & imgT^a_{\beta\alpha}\sqrt{p_1^+p_2^+}\chi^\dagger_{\lambda_2}\sigma^\perp.(\epsilon^\perp_\sigma)^*\chi_{\lambda_1}(-\frac{1}{2}C_A + C_f) \times \frac{g^2}{2(2\pi)^3}\int \frac{d^2k^\perp}{(k^\perp)^2} \\ & \int_0^{q^+} dk^+ \frac{1}{(p_1^+ - k^+)^2} \\ & = imgT^a_{\beta\alpha}\sqrt{p_1^+p_2^+}\chi^\dagger_{\lambda_2}\sigma^\perp.(\epsilon^\perp_\sigma)^*\chi_{\lambda_1} \\ & (-\frac{1}{2}C_A + C_f) \times \frac{g^2}{2\pi^2}(\frac{1}{p_2^+} - \frac{1}{p_1^+}) \ln\frac{\Lambda}{\mu}.\end{aligned} \tag{3.70}$$

The contribution from Fig. 3.8(b) is

$$\mathcal{M}_{8b} = 0. \tag{3.71}$$

The contribution from Fig. 3.8(c) is

$$\mathcal{M}_{8c} = 0. \tag{3.72}$$

Adding the various contributions we have,

$$\begin{aligned}\mathcal{M}_{2a} + \mathcal{M}_{2b} + \mathcal{M}_{8a} = \quad & imgT^a_{\beta\alpha}\sqrt{p_1^+ p_2^+}(\frac{1}{p_1^+} - \frac{1}{p_2^+})\chi^\dagger_{\lambda_2}\sigma^\perp.(\epsilon^\perp_\sigma)^*\chi_{\lambda_1} \\ & \times(-\frac{1}{2}C_A + C_f)\frac{g^2}{8\pi^2}\Big[2ln\frac{p_1^+ p_2^+}{\epsilon^2} - 3 + 2\Big]ln\frac{\Lambda}{\mu}.\end{aligned} \tag{3.73}$$

The contribution from Fig. 3.9(a) is

$$\mathcal{M}_{9a} = 0. \tag{3.74}$$

The contribution from Fig. 3.9(c) is

$$\begin{aligned}\mathcal{M}_{9c} \quad & = imgT^a_{\beta\alpha}\sqrt{p_1^+ p_2^+}\chi^\dagger_{\lambda_2}\sigma^\perp.(\epsilon^\perp_\sigma)^*\chi_{\lambda_1}(-)C_A \\ & \frac{1}{(p_1^+)^2}\frac{g^2}{2(2\pi)^3}\int\frac{d^2k^\perp}{(k^\perp)^2}\int_0^{p_1^+} dk^+ k^+\frac{(q^+ + k+)}{(q^+ - k+)^2}. \\ & = imgT^a_{\beta\alpha}\sqrt{p_1^+ p_2^+}\chi^\dagger_{\lambda_2}\sigma^\perp.(\epsilon^\perp_\sigma)^*\chi_{\lambda_1} \\ & \times(-)C_A\frac{g^2}{8\pi^2}\Big[\frac{4(q^+)^2}{(p_1^+)^2\epsilon} - \frac{3q^+}{(p_1^+)^2}ln\frac{q^+}{p_2^+} - \frac{2q^+}{p_1^+ p_2^+} + \frac{1}{p_1^+}\Big]\ln\frac{\Lambda}{\mu}.\end{aligned} \tag{3.75}$$

It is gratifying to see that the linear infrared divergence cancels between Figs. 3.3(a), 3.3(b) and 3.9(c).

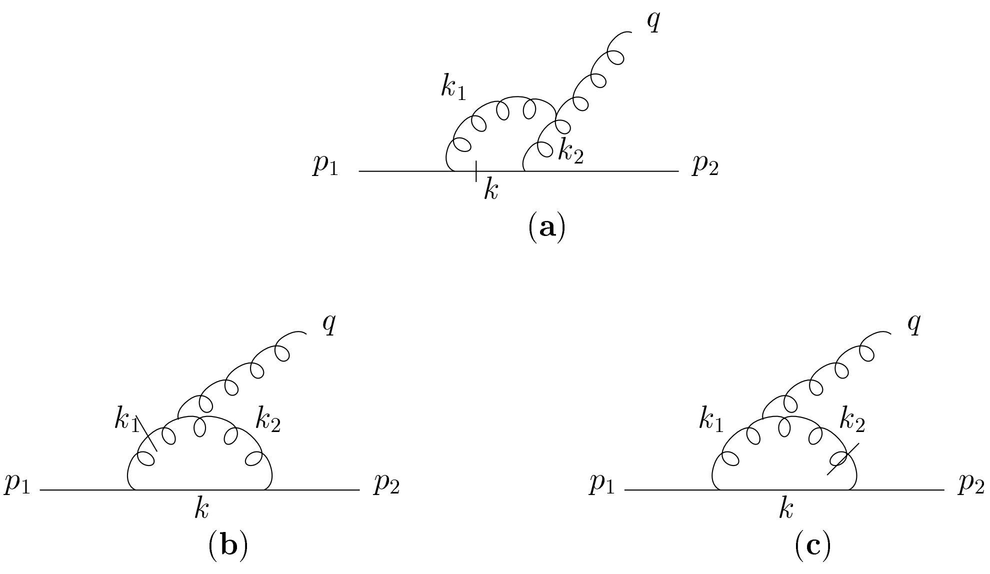

Fig. 3.9

The contribution from Fig. 3.9(b) is

$$\mathcal{M}_{9b} \quad = imgT^a_{\beta\alpha}\sqrt{p_1^+ p_2^+}\chi^\dagger_{\lambda_2}\sigma^\perp.(\epsilon^\perp_\sigma)^*\chi_{\lambda_1}(-)C_A\frac{g^2}{2(2\pi)^3}\frac{1}{(p_2^+)^2}\int\frac{d^2k^\perp}{(k^\perp)^2}$$

$$\int_0^{p_2^+} dk^+ k^+ \frac{(q^+ - k+)}{(q^+ + k+)^2}.$$
$$= imgT^a_{\beta\alpha}\sqrt{p_1^+ p_2^+}\chi^\dagger_{\lambda_2}\sigma^\perp.(\epsilon^\perp_\sigma)^*\chi_{\lambda_1}$$
$$\times(-)C_A\frac{g^2}{8\pi^2}\Big[\frac{3q^+}{(p_2^+)^2}ln\frac{p_1^+}{q^+} - \frac{2q^+}{p_1^+ p_2^+} - \frac{1}{p_2^+}\Big]\ln\frac{\Lambda}{\mu}. \tag{3.76}$$

Adding various contributions we have

$$\mathcal{M}_{3a} + \mathcal{M}_{3b} + \mathcal{M}_{9b} + \mathcal{M}_{9c} = imgT^a_{\beta\alpha}\sqrt{p_1^+ p_2^+}(\frac{1}{p_1^+} - \frac{1}{p_2^+})\chi^\dagger_{\lambda_2}\sigma^\perp.(\epsilon^\perp_\sigma)^*\chi_{\lambda_1}$$
$$\times(-)\frac{1}{2}C_A\frac{g^2}{8\pi^2}\Big[1 - 2ln\frac{p_1^+ p_2^+}{\epsilon^2} - 4ln\frac{q^+}{\epsilon}\Big]\ \ln\frac{\Lambda}{\mu}. \tag{3.77}$$

Coupling constant renormalization

In order to evaluate the contributions to coupling constant we have to multiply[30, 31] $\mathcal{M}_4$ and $\mathcal{M}_5$ by a factor of $\frac{1}{2}$. Thus adding the contributions, we have

$$\delta\mathcal{M}_{02} = \mathcal{M}_2 + \mathcal{M}_3 + \frac{1}{2}\mathcal{M}_4 + + \frac{1}{2}\mathcal{M}_5 + \mathcal{M}_6 + \mathcal{M}_7 + \mathcal{M}_8 + \mathcal{M}_9$$
$$= imgT^a_{\beta\alpha}\sqrt{p_1^+ p_2^+}(\frac{1}{p_1^+} - \frac{1}{p_2^+})\chi^\dagger_{\lambda_2}\sigma^\perp.(\epsilon^\perp_\sigma)^*\chi_{\lambda_1}$$
$$[\frac{11}{3}C_A - \frac{4}{3}N_f T_f]\frac{g^2}{16\pi^2}\ln\frac{\Lambda}{\mu}$$
$$+imgT^a_{\beta\alpha}\sqrt{p_1^+ p_2^+}(\frac{1}{p_1^+} - \frac{1}{p_2^+})\chi^\dagger_{\lambda_2}\sigma^\perp.(\epsilon^\perp_\sigma)^*\chi_{\lambda_1}$$
$$[2C_f + C_f]\frac{g^2}{8\pi^2}\ln\frac{\Lambda}{\mu}. \tag{3.78}$$

Recalling our previous discussion, we identify the first term in the above expression as the coupling constant correction and the second term as the "vertex mass" correction. Comparison with previous section shows that we get the same β function. An additional divergence however appears in the vertex as we anticipated. The "vertex mass" correction is

$$\delta m = \frac{3g^2}{8\pi^2}C_f\ln\frac{\Lambda}{\mu}. \tag{3.79}$$

This is exactly the mass correction expected in covariant theory for the mass counterterm. It is in fact surprising to see this factor emerging as the vertex counterterm in the light-front calculation since it is impossible to reproduce the covariant answer for the mass counterterm using the cutoffs we have employed in this paper. This aspect of regularization and renormalization seems worthy of further investigations in the future.

BIBLIOGRAPHY

[1] For a very early example of the “wrong sign” of charge renormalization see V.S. Vanyashin and M.V. Terent'ev, Sov. Phys. JETP, **21**, 375 (1965).

[2] G. 't Hooft, hep-th/9808154.

[3] D.J. Gross and F. Wilczek, Phys. Rev. Lett. **30**, 1343 (1973).

[4] H. David Politzer, Phys. Rev. Lett. **30**, 1346 (1973).

[5] I.B. Khriplovich, Sov. J. Nuc. Phys. **10**, 235 (1970).

[6] J. Frenkel and J.C. Taylor, Nucl. Phys. **B109**, 439 (1976).

[7] T. Appelquist, M. Dine, and I.F. Muzinich, Phys. Lett. **B69**, 231 (1977).

[8] T.D. Lee, *Particle Physics and Introduction to Field Theory* (Harwood Academic Publishers, New York, 1981).

[9] For a detailed discussion of gluon propagator in axial gauge see G. B. West, Phys. Rev. **D27**, 1878 (1983).

[10] C. B. Thorn, Phys. Rev. **D20**, 1934 (1979).

[11] G. Curci, W. Furmanski, and R. Petronzio, Nucl. Phys. **175**, 27 (1980).

[12] S.J. Brodsky, F.E. Close and J.F. Gunion, Phys. Rev. **D8**, 3679 (1973).

[13] S. Mandelstam, Nucl. Phys. **B213**, 140 (1983).

[14] G. Leibbrandt, Phys. Rev. **D29**, 1699 (1984).

[15] D.M. Capper, J.J. Dulwych and M.J. Litvak, Nucl. Phys. **B241**, 463 (1984).

[16] H.C. Lee and M.S. Milgram, Nucl. Phys. **B268**, 543 (1986).

[17] A. Bassetto, G. Nardulli, and R. Soldati, *Yang-Mills theories in algebraic non-covariant gauges*, (World Scientific, Singapore, 1991).

[18] For an attempt towards the implementation of Mandelstam-Leibbrandt prescription in light-front bound state equation see H.H. Liu and D.E. Soper, Phys. Rev. D**48**, 1841 (1993).

[19] K. G. Wilson, “Light front QCD”, unpublished, K.G. Wilson *et al.*, Phys. Rev. D**49**, 6720 (1994).

[20] R.K. Ellis, H. Georgi, M. Machacek, H.D. Politzer, and G.G. Ross, Nucl. Phys. **B152**, 285 (1979).

[21] Yu.L. Dokshitzer, D.I. Dyakonov, and S.I. Troyan, Phys. Rep. **C58**, 269 (1980).

[22] S.D. Drell, D.J. Levi, and T.-M. Yan, Phys. Rev. Lett. **22**, 744 (1969); Phys. Rev. **187**, 2159 (1969); **D1**, 1035 (1970); **D1**, 1617 (1970).

[23] J.D. Bjorken, J.B. Kogut, and D.E. Soper, Phys. Rev.**D3**, 1382 (1971).

[24] S.J. Brodsky and G.P. Lepage, in *Perturbative Quantum Chrodynamics*, edited by A.H. Mueller (World Scientific, Singapore, 1989), p93 and references therein.

[25] St. Glazek, A. Harindranath, S. Pinsky, J. Shigemitsu, and K. Wilson, Phys. Rev. D47, 1599 (1993).

[26] R.J. Perry, Phys. Lett. **B300**, 8 (1993).

[27] W.-M. Zhang and A. Harindranath, Phys. Rev. D**48**, 4903 (1993).

[28] A. Harindranath and Rajen Kundu, Int. J. Mod. Phys. A **13**, 4591 (1998).

[29] W.-M. Zhang and A. Harindranath, Phys. Rev. D**48**, 4881 (1993).

[30] J.D. Bjorken and S.D. Drell, *Relativistic Quantum Mechanics*, (McGraw-Hill, New York, 1964).

[31] W. Heitler, *The Quantum Theory of Radiation*, (The Oxford University Press, London, 1936).